

NASA TECHNICAL  
MEMORANDUM



NASA TM X-1211

NASA TM X-1211

FACILITY FORM 602

N66-17890

(ACCESSION NUMBER) \_\_\_\_\_ (THRU) \_\_\_\_\_

14 \_\_\_\_\_ 1 \_\_\_\_\_

(PAGES) \_\_\_\_\_ (CODE) \_\_\_\_\_

TMX-1211 \_\_\_\_\_ 32 \_\_\_\_\_

(NASA CR OR TMX OR AD NUMBER) \_\_\_\_\_ (CATEGORY) \_\_\_\_\_

GPO PRICE \$ \_\_\_\_\_

CFSTI PRICE(S) \$ 1.00

Hard copy (HC) \_\_\_\_\_

Microfiche (MF) .50

ff 653 July 85

# EXPERIMENTAL INVESTIGATION TO DETERMINE UTILITY OF TENSION SHELL CONCEPT

*by W. Jefferson Stroud and George W. Zender*

*Langley Research Center*

*Langley Station, Hampton, Va.*

EXPERIMENTAL INVESTIGATION TO DETERMINE  
UTILITY OF TENSION SHELL CONCEPT

By W. Jefferson Stroud and George W. Zender

Langley Research Center  
Langley Station, Hampton, Va.

NATIONAL AERONAUTICS AND SPACE ADMINISTRATION

EXPERIMENTAL INVESTIGATION TO DETERMINE  
UTILITY OF TENSION SHELL CONCEPT

By W. Jefferson Stroud and George W. Zender  
Langley Research Center

SUMMARY

An experimental investigation of shell configurations was conducted to determine the utility of the tension shell concept proposed in NASA TN D-2675 for application to entry vehicles. A total of ten plastic models comprising three shapes were considered, and the results confirm the utility of the proposed concept.

INTRODUCTION

The mathematical development of a high-drag tension shell configuration for entry into thin planetary atmospheres is presented in reference 1. Linear membrane theory is used in the analysis to derive shapes of shells of revolution which have only nonnegative stresses when the shells are subjected to axisymmetric aerodynamic loadings. Reference 2 indicates that, in addition to desirable aerodynamic characteristics (high drag), the tension shell offers advantageous ratios of payload to total weight, particularly at low values of the ballistic coefficient. The tension shell concept permits designing the shell wall on the basis of the ultimate tensile strength whereas the maximum allowable stress for more conventional entry-body configurations is usually limited by buckling considerations. In the tension shell structure considered herein, compressive forces are concentrated in a ring at the aft end of the shell - a desirable feature for efficient design.

In order to provide an early assessment of the structural response of the tension shell structure, several plastic models were subjected to static loads which approximate the pressure loadings that would act on a vehicle during atmospheric entry. Results of this experimental investigation are presented herein.

SYMBOLS

The physical quantities defined in this paper are given both in the U.S. Customary Units and in the International System of Units (SI) (ref. 3). The appendix presents factors relating these two systems of units.

|            |  |
|------------|--|
| r          | radius, inches (cm)  |
| s          | distance along periphery, inches (cm)                            |
| t          | thickness of shell wall, inches (cm)                             |
| z          | height, inches (cm)  |
| $N_\theta$ | circumferential in-plane stress resultant, pounds per inch (N/m) |
| $N_\phi$   | meridional in-plane stress resultant, pounds per inch (N/m)      |

### MODELS

The tension shell configuration resulting from membrane analysis presented in reference 1 has the general shape shown in figure 1. The figure also indicates the directions of the stress resultants  $N_\theta$  and  $N_\phi$ .

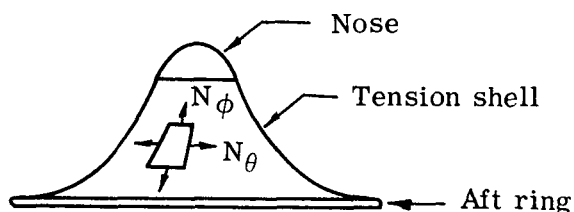


Figure 1.- General shape of tension shell.

The coordinates of the shell profile are dependent upon the axisymmetric prescribed loading and are given in reference 1 for various values of the stress ratio  $N_\theta/N_\phi$ . For each particular shell configuration the stress ratio is prescribed as constant throughout the shell. The attention of this study is centered upon the shell rather than upon the nose or aft-ring design.

The two tension shell shapes shown in figure 5 of reference 1 were selected for experimental study. One tension shell shape, designated the uniform pressure shape, is designed to have zero circumferential stress when subjected to a uniform pressure loading. The other tension shell shape, designated the Newtonian pressure shape, is designed to have zero circumferential stress when the aerodynamic loading is a Newtonian pressure distribution (see eq. (9) of ref. 1). Although the uniform and Newtonian pressure distributions differ considerably, the difference in geometry of the two configurations is not large. Details of the method of loading for this experimental study are given subsequently. The loading which was applied to all models considered herein was a uniform pressure distribution. The Newtonian pressure shape is thus subjected to an off-design load and therefore develops a compressive stress resultant in the circumferential direction.

In addition to the two tension shell shapes, a conical shape was included for comparison. The conical shape also develops a compressive stress resultant in the circumferential direction under a uniform pressure loading.

Three models with the uniform pressure shape, four with the Newtonian pressure shape, and three with the conical shape were considered in the experimental investigation. The overall dimensions of the models are similar and are shown in figure 2. The base diameters are identical and the drag coefficients are nearly the same.

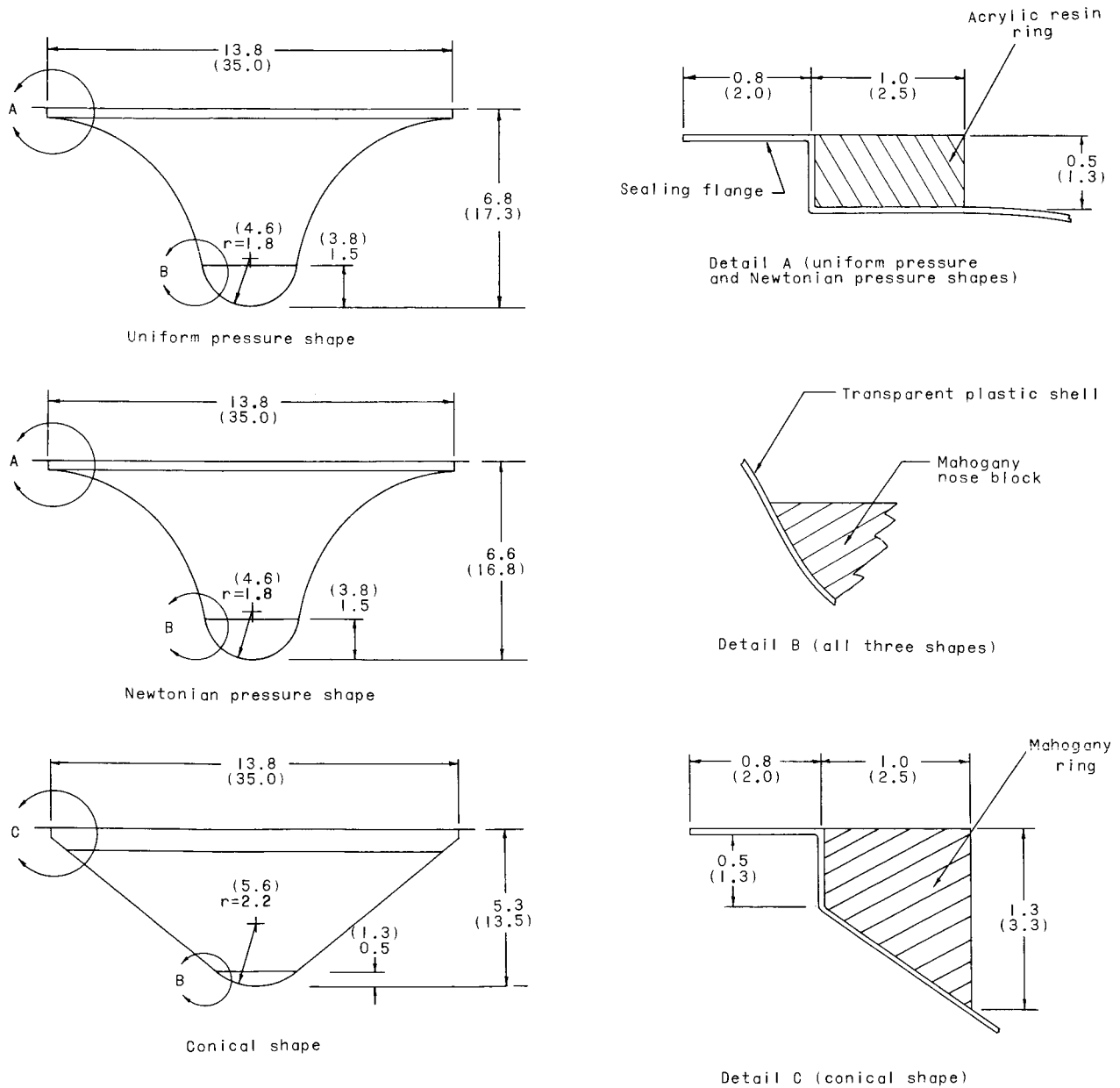


Figure 2.- Dimensions of the three configurations. Measurements are given in inches and parenthetically in centimeters.

Models having the three shapes were made from plastic (cellulose acetate butyrate) sheets of various thicknesses within the nominal range from 0.03 to 0.08 inch (0.8 to 2.0 mm). Shaping a model consisted of radiantly heating a plastic sheet to a moderately elevated temperature and drawing it over a male mold. The final step of the drawing procedure consisted of evacuating the air space between the model and the mold. After the model had cooled considerably, it was removed from the mold. The coordinates of the three molds used to make the three configurations are given in table 1. This method of shaping produced a model which did not quite fit the mold after the plastic cooled completely. The stretching which accompanied the shaping also caused the thickness of the shell wall to decrease from the base toward the nose. Table 2 gives the thickness variations for the ten models.

After the plastic sheet was shaped into the proper configuration, an acrylic resin ring was bonded to the base of models having the uniform pressure and Newtonian pressure shapes and a mahogany ring was bonded to the base of models having the conical shape. A mahogany block was inserted in the nose of each model for the purpose of distributing a vertical load, applied through a steel eye bolt, into the shell wall. A polyester adhesive was used as the bonding agent to attach both the ring and the block to each shell. The two types of rings and the nose block are shown in figure 2.

## APPARATUS AND TESTS

The sealing flange of each model (see fig. 2) was taped to a smooth flat metal surface as shown in figure 3. The metal surface contained one port to allow a vacuum pump to evacuate the interior of the model. Another port was connected to a mercury manometer for measuring the interior pressure. The difference between the interior pressure and the atmospheric pressure acting on the outside of the shell constituted the uniform pressure loading on the shell. In addition, a vertical tensile force was applied to the model by a hydraulic jack attached to an overhead framework. The vertical load was measured with a load cell unit between the jack and an eye bolt attached to the model. The hydraulically applied load and the pressure difference were scheduled so that the upward load at the nose just balanced the downward component of the pressure loading. Thus, no vertical force existed between the model base and the metal surface. The vertical load simulates the inertial loading of the entry vehicle, and the pressure loading approximates the aerodynamic loading. A Tuckerman optical strain gage was mounted on the shell to measure circumferential strain at about midheight of the model. The test setup is shown in figure 3.

The test procedure consisted of subjecting the model to various differential pressures in prescribed increments along with corresponding values of vertical load to balance the vertical component of the pressure loading. All models except one were loaded

until either buckling or fracture occurred. The maximum load applied to the remaining model was not sufficient to buckle or to fracture that model.

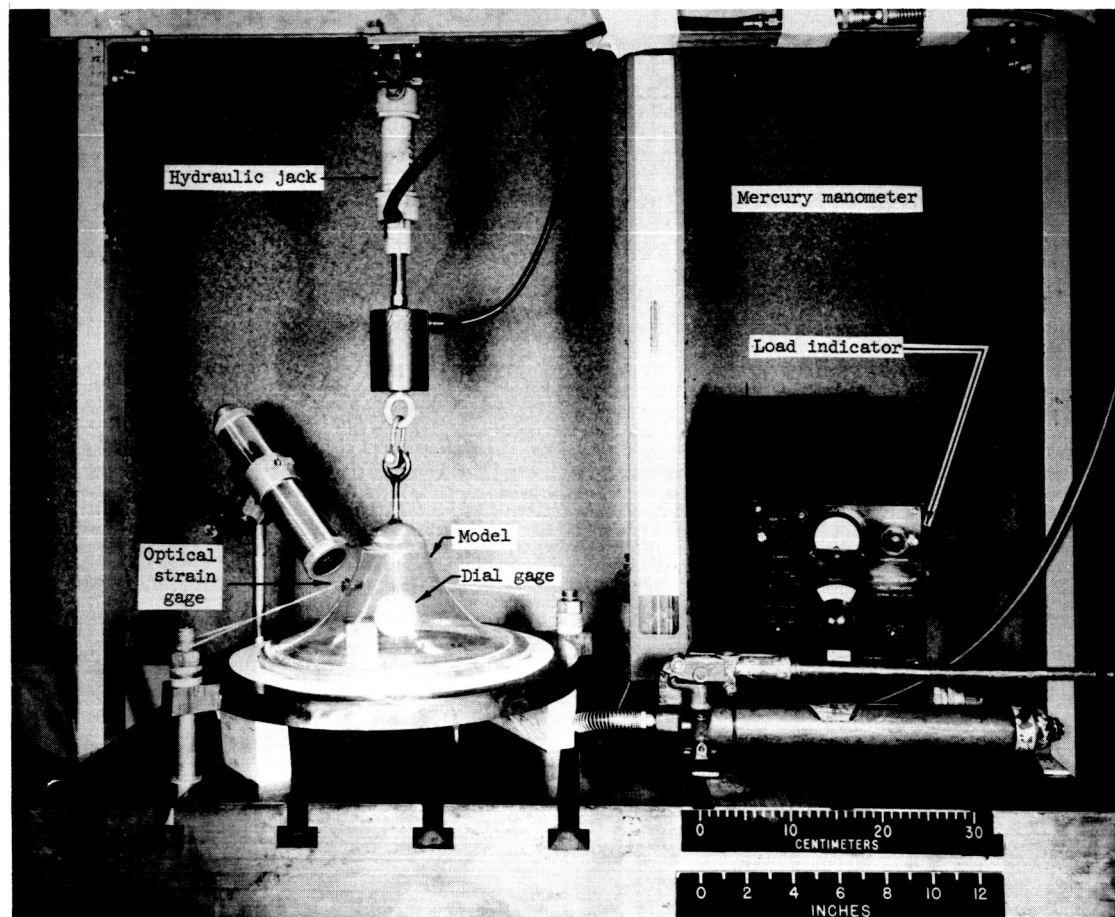


Figure 3.- Test setup for entry-vehicle model.

L-64-10500.1

## RESULTS AND DISCUSSION

The results of the investigation are shown in figure 4 for all three shapes. The abscissa scale is the average wall thickness of the model, and the ordinate scales are the pressure difference and the vertical load acting on the model. The open symbols indicate the loads at which buckling of the type shown in figure 5 occurred. The curve faired through the square symbols is for models having the Newtonian pressure shape, and the curve through the triangular symbols is for models having the conical shape. Buckling might be expected for the models having these two shapes inasmuch as these shapes were not designed to be tension shells when subjected to the test loading.

The buckling load was determined from plots of strain-gage data and from visual observations. Load-strain plots such as the one in figure 6 showed a departure from linearity near the onset of buckling. In some tests, extraneous buckling occurred in

portions of the model at lower loads than those required for buckling in the region of the strain gage. In other tests, the load necessary to hold the strain gage to the model precipitated buckling in the region of the strain gage. For example, the thinnest conical model was tested without strain-gage instrumentation because the strain-gage attachment load alone was sufficient to produce a large deformation. For these reasons the buckling load was determined from both the visual observations and strain-gage data.

Two of the ten models did not buckle. (See solid symbols in fig. 4.) Both of these models had the uniform pressure shape – a tension shell shape designed to have zero circumferential stress for the test loading. The upper solid symbol in figure 4 indicates that 6.9 psi (47.6 kN/m<sup>2</sup>) is the pressure difference and 750 pounds (3.3 kN) is the vertical load at which the model having an average wall thickness of 0.0307 inch (0.0780 cm) fractured in tension. The lower solid symbol indicates that 5.2 psi (35.8 kN/m<sup>2</sup>) is the largest pressure difference and 570 pounds (2.5 kN) is the largest vertical load to which the model having an average wall thickness of 0.0249 inch (0.0633 cm) was subjected. This model neither fractured nor buckled at those loading conditions. The lowest circular symbol in figure 4 shows the loading conditions at which buckling occurred on the thinnest of the models having the uniform pressure shape. The buckling may have been caused by irregularities and/or deformations under load which are not accounted for in the theory (ref. 1).

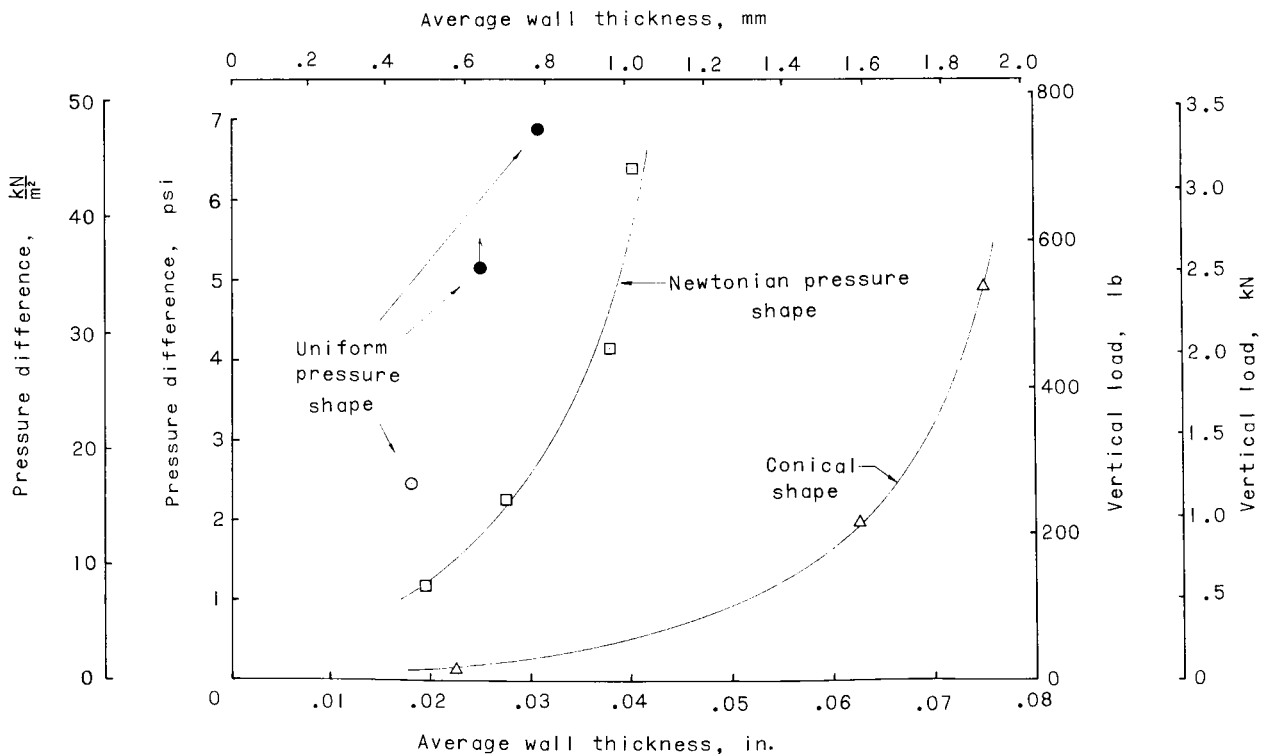
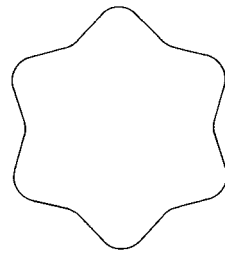
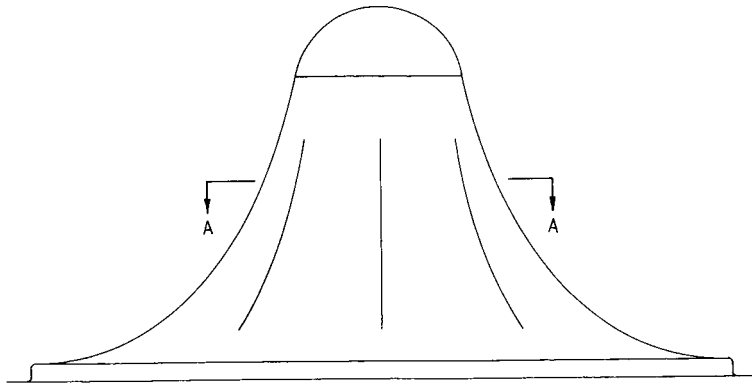


Figure 4.- Pressure difference and corresponding vertical load as functions of average wall thickness for three model configurations.



Section A-A

Figure 5.- Buckle pattern (exaggerated).

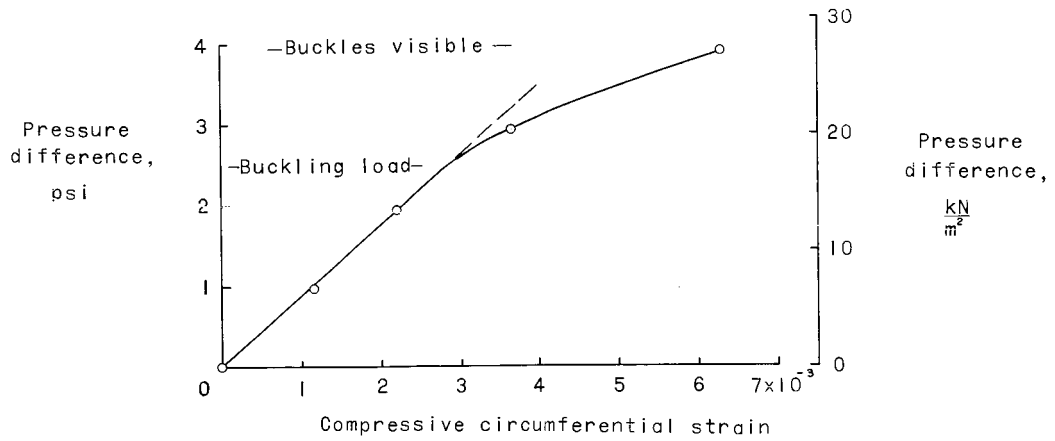


Figure 6.- Pressure difference as a function of circumferential strain for uniform pressure model having an average wall thickness of 0.0182 inch (0.0462 cm).

The results show that to prevent buckling at a given uniform pressure loading, the conical models would have required a wall thickness about two and one-half times that of the uniform pressure models, and the Newtonian pressure models would have required a wall thickness about one and one-half times that of the uniform pressure models. It is noteworthy that the coordinates for the models having a Newtonian pressure shape do not differ substantially from those for the models having a uniform pressure shape; nevertheless, the small differences which do exist appear to make a significant difference in buckling strength. It is possible to configure a tension shell which has tension in the circumferential direction as well as in the meridional direction and thereby provide for a margin against compressive stress due to inaccuracies in final shape and nonaxisymmetric loading conditions.

Langley Research Center,

National Aeronautics and Space Administration,

Langley Station, Hampton, Va., November 12, 1966.

## APPENDIX

### CONVERSION OF U.S. CUSTOMARY UNITS TO SI UNITS

The International System of Units (SI) was adopted by the Eleventh General Conference on Weights and Measures, Paris, October 1960, in Resolution No. 12 (ref. 3). Conversion factors for the units used herein are given in the following table:

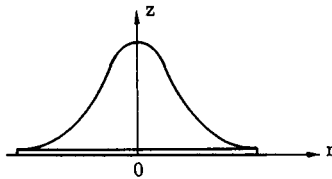
| Physical quantity  | U.S. Customary Unit | Conversion factor (*) | SI Unit                                      |
|--------------------|---------------------|-----------------------|--|
| Length . . . . .   | in.                 | 0.0254                | meters (m)                                   |
| Force . . . . .    | lbf                 | 4.448                 | newtons (N)                                  |
| Pressure . . . . . | lbf/in <sup>2</sup> | $6.89 \times 10^3$    | newtons per square meter (N/m <sup>2</sup> ) |

\* Multiply value given in U.S. Customary Unit by conversion factor to obtain equivalent value in SI Unit.

## REFERENCES

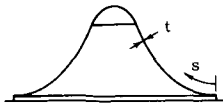
1. Anderson, Melvin S.; Robinson, James C.; Bush, Harold G.; and Fralich, Robert W.:  
A Tension Shell Structure for Application to Entry Vehicles. NASA TN D-2675,  
1965.
2. Anderson, Roger A.: Structures Technology - 1964. Astronaut. Aeron., vol. 2,  
no. 12, Dec. 1964, pp. 14-20.
3. Mechtly, E. A.: The International System of Units - Physical Constants and  
Conversion Factors. NASA SP-7012, 1964.

TABLE 1.- COORDINATES OF THE MOLDS USED FOR THE THREE CONFIGURATIONS



| r        |      | z for -                        |       |                                  |       |                       |       |
|----------|------|--------------------------------|-------|----------------------------------|-------|-----------------------|-------|
|          |      | Uniform pressure configuration |       | Newtonian pressure configuration |       | Conical configuration |       |
| in.      | cm   | in.                            | cm    | in.                              | cm    | in.                   | cm    |
| 6.9      | 17.5 | 0                              | 0     | 0                                | 0     | 0                     | 0     |
| 6.9      | 17.5 | .45                            | 1.14  | .45                              | 1.14  | .50                   | 1.27  |
| 6.5      | 16.5 | .49                            | 1.24  | .47                              | 1.19  | .82                   | 2.07  |
| 6.0      | 15.2 | .58                            | 1.47  | .55                              | 1.40  | 1.21                  | 3.07  |
| 5.5      | 14.0 | .73                            | 1.85  | .73                              | 1.85  | 1.60                  | 4.07  |
| 5.0      | 12.7 | .97                            | 2.46  | 1.02                             | 2.59  | 1.99                  | 5.07  |
| 4.5      | 11.4 | 1.28                           | 3.25  | 1.41                             | 3.58  | 2.39                  | 6.07  |
| 4.0      | 10.2 | 1.67                           | 4.24  | 1.91                             | 4.85  | 2.78                  | 7.07  |
| 3.5      | 8.9  | 2.17                           | 5.51  | 2.51                             | 6.38  | 3.18                  | 8.07  |
| 3.0      | 7.6  | 2.77                           | 7.04  | 3.20                             | 8.13  | 3.57                  | 9.07  |
| 2.5      | 6.4  | 3.51                           | 8.92  | 4.00                             | 10.16 | 3.96                  | 10.06 |
| 2.0      | 5.1  | 4.50                           | 11.43 | 4.88                             | 12.40 | 4.36                  | 11.07 |
| 1.5      | 3.8  | 5.91                           | 15.01 | 5.80                             | 14.73 | 4.75                  | 12.07 |
| 1.0      | 2.5  | 6.44                           | 16.36 | 6.29                             | 15.98 | 5.07                  | 12.88 |
| .5       | 1.3  | 6.68                           | 16.97 | 6.52                             | 16.56 | 5.25                  | 13.34 |
| 0 (Nose) | 0    | 6.75                           | 17.14 | 6.59                             | 16.74 | 5.30                  | 13.46 |

TABLE 2.- THICKNESS VARIATIONS FOR MODELS



(a) Models with uniform pressure shape

| s   |      | t for model with -                    |        |                                       |        |                                       |        |
|-----|------|---------------------------------------|--------|---------------------------------------|--------|---------------------------------------|--------|
|     |      | Average t = 0.0182 in.<br>= 0.0462 cm |        | Average t = 0.0249 in.<br>= 0.0633 cm |        | Average t = 0.0307 in.<br>= 0.0780 cm |        |
| in. | cm   | in.                                   | cm     | in.                                   | cm     | in.                                   | cm     |
| 1.0 | 2.5  | 0.0210                                | 0.0533 | 0.0310                                | 0.0787 | 0.0343                                | 0.0871 |
| 2.0 | 5.1  | .0194                                 | .0493  | .0289                                 | .0734  | .0341                                 | .0866  |
| 3.0 | 7.6  | .0190                                 | .0483  | .0272                                 | .0692  | .0324                                 | .0823  |
| 4.0 | 10.2 | .0174                                 | .0442  | .0247                                 | .0629  | .0306                                 | .0777  |
| 5.0 | 12.7 | .0163                                 | .0414  | .0203                                 | .0516  | .0283                                 | .0719  |
| 5.8 | 14.7 | .0164                                 | .0417  | .0174                                 | .0442  | .0243                                 | .0617  |

(b) Models with Newtonian pressure shape

| s   |      | t for model with -                    |        |                                       |        |                                       |        |                                      |        |
|-----|------|---------------------------------------|--------|---------------------------------------|--------|---------------------------------------|--------|--------------------------------------|--------|
|     |      | Average t = 0.0196 in.<br>= 0.0498 cm |        | Average t = 0.0277 in.<br>= 0.0703 cm |        | Average t = 0.0379 in.<br>= 0.0963 cm |        | Average t = 0.0401 in.<br>= 0.102 cm |        |
| in. | cm   | in.                                   | cm     | in.                                   | cm     | in.                                   | cm     | in.                                  | cm     |
| 1.0 | 2.5  | 0.0230                                | 0.0584 | 0.0326                                | 0.0828 | 0.0508                                | 0.1290 | 0.0468                               | 0.1189 |
| 2.0 | 5.1  | .0222                                 | .0564  | .0314                                 | .0798  | .0456                                 | .1158  | .0416                                | .1057  |
| 3.0 | 7.6  | .0205                                 | .0521  | .0291                                 | .0739  | .0408                                 | .1036  | .0419                                | .1064  |
| 4.0 | 10.2 | .0186                                 | .0472  | .0268                                 | .0681  | .0347                                 | .0881  | .0398                                | .1011  |
| 5.0 | 12.7 | .0171                                 | .0434  | .0242                                 | .0615  | .0288                                 | .0732  | .0360                                | .0914  |
| 5.8 | 14.7 | .0162                                 | .0411  | .0223                                 | .0566  | .0264                                 | .0671  | .0344                                | .0874  |

(c) Models with conical shape

| s   |      | t for model with -                    |        |                                       |        |                                       |        |
|-----|------|---------------------------------------|--------|---------------------------------------|--------|---------------------------------------|--------|
|     |      | Average t = 0.0225 in.<br>= 0.0571 cm |        | Average t = 0.0627 in.<br>= 0.1592 cm |        | Average t = 0.0751 in.<br>= 0.1909 cm |        |
| in. | cm   | in.                                   | cm     | in.                                   | cm     | in.                                   | cm     |
| 1.0 | 2.5  | 0.0227                                | 0.0577 | 0.0635                                | 0.1613 | 0.0771                                | 0.1958 |
| 2.0 | 5.1  | .0222                                 | .0564  | .0628                                 | .1595  | .0753                                 | .1913  |
| 3.0 | 7.6  | .0228                                 | .0579  | .0628                                 | .1595  | .0746                                 | .1895  |
| 4.0 | 10.2 | .0226                                 | .0574  | .0626                                 | .1590  | .0744                                 | .1890  |
| 5.0 | 12.7 | .0218                                 | .0554  | .0619                                 | .1572  | .0744                                 | .1890  |